

Stress Concentration Analysis of Grain Refinement in Rheology Casting Process

양자오*(부산대 대학원 정밀기계공학과), 서판기(부산대 대학원 정밀기계공학과), 고재홍(부산대 대학원 정밀기계공학과), 정용식(부산대 대학원 정밀기계공학과), 강충길(부산대 기계공학부)

Z. Yang, P.K. Seo, J.H. Ko, Y.S. Jung and C.G. Kang

ABSTRACT

The mechanics of the dendrite fragmentation is a very important aspect of grain refinement in rheocasting. In this work, the stress field of the dendrite stirred in the semisolid slurry was simulated by Matlab 6.0 software. The result shows that stress concentration at the root of the dendrite arms is great enough to cause plastic deformation though the agitation is moderate. Accordingly, dendrite fragmentation was suggested to be caused by fractured after fatigue erosion.

Key Words semisolid metal process, grain refinement, stress concentration, FEM.

1. 서론

Grain refinement in stirred semisolid suspensions is an interesting but stubborn subject [1,2]. Because direct observation is unavailable, this problem is still far from being completely understood though it has been investigated for thirty years [3-8]. It is generally accepted that grain refinement in stirred semisolid slurries is caused by dendrite fragmentation. Divergence lies in how the dendrite arms fracture. There are three major hypotheses [1,2]: 1. The dendrite arms are sheared off by liquid flow; 2. The roots of the dendrite arms are ruptured after being thinned by ripening; and 3. Repeated plastic bending creates numerous dislocations at the roots of the dendrite arms, and these dislocations will form subgrain boundaries by recrystallization. If the subgrain boundary energy is more than twice the solid-liquid interfacial energy, they will be wet by liquid. It is reasonable that dendrite arms can be plastically bent and sheared off in fluids with high shear rate. But the explanations of dendrite fragmentation in fluids with low shear rate are not convincing. Can slow liquid flow create enough force to bend the dendrite arms plastically? Is there enough time for ripening to act in a continuously stirred cooling process?

In recent year, Mullis [4] has directly observed an NH_4Cl dendrite fractured in a semisolid $\text{NH}_4\text{Cl-H}_2\text{O}$

system stirred at a very low shear rate, 3 s^{-1} . This could be a good proof of the hypothesis of breaking after repeated bending. But Mullis gave a crystallographic explanation. What led him to that conclusion is Pilling's calculation [9], which showed it is difficult for a dendrite arm to be bent plastically in a slowly flowing liquid. However it seems that Pilling has missed a very important factor, stress concentration.

This work reexamines Pilling's work by including stress concentration. The results confirm that stress concentration is great enough to cause plastic deformation at the roots of the dendrite arms. So a hypothesis, fracture after fatigue, is suggested.

2. A plane stress model

In order to facilitate the calculation of the stress field of a equiaxed dendrite in a stirred Al based semisolid slurry, the dendrite arm and the primary dendrite stem are simplified to two perpendicular cylinders with the diameters $2R_1=40 \mu\text{m}$ and $2R_2=70 \mu\text{m}$, respectively, as shown in Fig.1. A flow with a uniform velocity is assumed to be perpendicular to the arm. Because stress concentration is sensitive to the configuration of the root, the contour of the neck is described by the tip of an ellipse based on the microstructures shown in

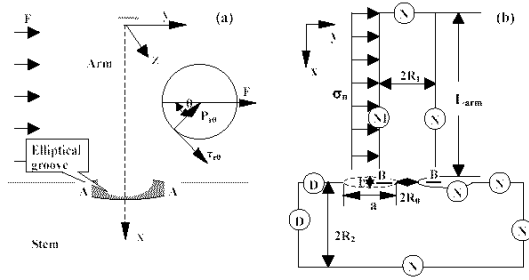


Fig.1 (a) Spatial sketch of the simplified dendrite arm in a flow. (b) 2-dimensional model of the dendrite. N: Neumann boundary condition with a free surface, NI: Neumann boundary condition with a loaded surface. D: Dirichlet boundary condition with no displacement. A-A and B-B is the cross sections at the necking of the root in 3D model and 2D

reference 5 and 6. The curvature at the necking is controlled by the aspect ratio of the ellipse, a/b , as shown in Fig.1(b). The larger the aspect ratio, a/b , the smaller the radius of the curvature.

In order to facilitate the calculation and to improve the accurate, a 2-D model was used to substitute the 3-D model. Coordinates are chosen with the x-axis parallel to the dendrite arm and the y-axis parallel to the flow of the liquid, as shown in Fig.1. It is clear that the sum of the components of the fluid force in the z-axis is zero, so a plane stress model is formed as following.

The Reynolds number of a flowing aluminum liquid is calculated by formula 1:

$$Re = \frac{V \cdot \rho \cdot 2 \cdot R_1}{\eta} \quad (1),$$

where Re is Reynolds number, V , η and ρ are velocity, viscosity and density of the flowing liquid, respectively. As shown in Table 1, the Reynolds number of the liquid is small, so the turbulence on the downstream side of the arm is neglected in this work. According to the reference 9, the fluid force per unit length, F_y , can be calculated by:

$$F_y = 3\pi\eta v \quad (2).$$

Because the fluid force acting on the arm is independent of the radius of the arm, a rectangular plate with a normal stress, σ_n , acting on the upstream side, as shown in Fig.1(b), must be equivalent to the arm with the combined force of shearing stress and pressure acting on its upstream semi-cylindrical surface. Because the thickness of the 2D arm is

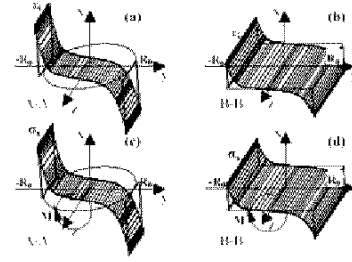


Fig.2 Sketch of the distributions of the strains and stresses on the section A-A, (a), (c) and on the section B-B, (b), (d).

arbitrary, it is set to $2R_0$, the minimum diameter of the neck so that the entire dendrite can be converted to a plate with the same thickness. The normal stress, σ_n , acting on the upstream face is calculated by:

$$\sigma_n = F_y / 2R_0 \quad (3).$$

The radii at the neck vary along the x-axis. In order to convert the concave root to 2D mode, the coaxial circles are substituted by a series of rectangles with the same thickness, $2R_0$. The circular cross section A-A of the necking then becomes a square cross section B-B with the size of $2R_0 \times 2R_0$ at the necking of the 2D arm, as shown in Fig.2. Because the deviation of the calculation is inevitable, an approximate adjustment is made. It is reasonable to assume that the strain components in each axis on section A-A, ε_{Ai} , is proportional to those on section B-B, ε_{Bi} [10]:

$$\varepsilon_{Ai}(y) = N\varepsilon_{Bi}(y) \quad (7)$$

Based on Hooke's law, the relationship between the stress components in the x-axis on section A-A, $\sigma_{Ax}(y)$, and on section B-B, $\sigma_{Bx}(y)$, can be described as equation 8:

$$\sigma_{Ax}(y) = \frac{(1-\nu) \cdot E}{1-\nu-2\nu^2} \left[\varepsilon_{Ax}(y) + \frac{\nu}{1+\nu} \cdot (\varepsilon_{Ay}(y) + \varepsilon_{Az}(y)) \right] = N \cdot \sigma_{Bx}(y) \quad (8),$$

where E is Young's modulus and ν is Poisson's ratio. The components of stresses in the y-axis on sections A-A and B-B can be calculated in the same way. According to Fig.3(a), $\sigma_{Bx}(y)$ could be described approximately as:

$$\sigma_{Bx}(y) = Ky^4 \quad (9),$$

where K is a constant. Because the stresses on

Table 1 Parameters of Aluminum for simulation [9].

| ρ , kg m ⁻³ | η , kg m ⁻¹ s ⁻¹ | V , m s ⁻¹ | Re | E, GPa | σ , MPa | ν | σ , N m ⁻¹ | Lm, J kg ⁻¹ | Tm, K | Γ , K μ m |
|-----------------------------|---------------------------------------------|-------------------------|-----|--------|----------------|-------|------------------------------|------------------------|-------|----------------------|
| 2.7E3 | 3.12E-3 | 4E-2 | 1.4 | 0.7 | 6.5 | 0.3 | 868 E-3 | 397 E3 | 933 | 0.77 |

section A-A and B-B must create equal moment about the z-axis to counteract the moment about the z-axis created by the fluid force, an equation can be obtained as following:

$$M = 2 \int_0^{R_0} \sigma_{Ax}(y) \cdot 2\sqrt{R_0^2 - y^2} \cdot y dy$$

$$= 2 \int_0^{R_0} \sigma_{Bx}(y) \cdot 2R_0 \cdot y dy \quad (10).$$

N is calculated to be 8.2. The stress field over other sections near section B-B can also be adjusted in this way. The difference is that N will decrease because the ratio between the integrated areas of the rectangle and circle is changed.

Boundary condition in Fig.1(b) is simplified as following. Assume that one end of the stem is fixed. Its surfaces are described by the Dirichlet boundary condition with no displacement. The upstream face of the dendrite arm is the only surface that is compressed by flowing liquid. It can be described as a Neumann boundary condition with a normal stress acting on its surface. The other surfaces of the dendrite, including the two grooves, are supposed to be free. They are described as the Neumann boundary condition with free surface. Inputting the plane stress model, the boundary conditions and the parameters in Table 1 into the Partial Differential Equation Tool Box in MatLab software, the stress field of the aluminum dendrites can be calculated.

3. Result

In this simulation, the minimum diameter of the neck at the root, $2R_0$, is fixed at $10 \mu\text{m}$ to facilitate comparison. Fig.3(b) shows the magnified plot of the von Mises effective stress σ_{Be} at the root of a 2D dendrite arm of $250 \mu\text{m}$ long, which suffers a fluid force of $12\text{E-}4\text{N/m}$. Stress concentration on the skin of the neck is great. Adjusted by equation 8, the maximum effective von Mises stress on section A-A is 4.6MPa , which is close to the yield strength. In Pilling's work [9], the maximum stress on the skin of the neck is lower than one tenth of the yield strength under this condition.

The theoretical formula to estimate the stress concentration factor of an elliptic hole is [10]:

$$K_t = 1 + 2a/b \quad (11).$$

Compared with Pilling's work, the result basically agrees with formula 11. The negative deviation is ascribed to the fact that the computer is not powerful enough especially when the radius of curvature of the neck decreases.

4. Discussion

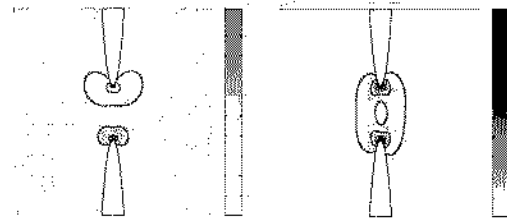


Fig.3 Magnified stress field at the root of the 2D dendrite arm when bending force is $12\text{E-}4 \text{N m}^{-1}$, the length of the dendrite arm is $250 \mu\text{m}$, and the aspect ratio of the ellipse is 10. (a) The component of the stress in x-axis, σ_{xx} . (b) The von Mises effective stress, σ_e .

Doherty et al [11] bent aluminum single crystals at a temperature near the melting point and found that high angle subgrain boundaries can be created by plastic bending, which means wetting is possible. But the dendrite arms of the primary dendrites are usually so short that only in the semisolid slurries stirred at a very high shear rate can they be bent plastically [12]. When the shear rate is low, the dendrite arms must be ruptured in another gradual way. It is well known that specimens in fatigue test fracture under the load much smaller than their yield strength. Cracks initiate on the surface where stress concentration occurs, and will propagate with the help of stress concentration [13]. In stirred semisolid slurries, dendrites roll and collide with each other. It is easy to associate the gradual rupture of the dendrite arms with fatigue.

When dendrite arms are bent by a cycling load, slip band extrusions and intrusions will occur on the skin at the root of the arms due to stress concentration, as shown in Fig.4. The radii of the curvature of the slip band extrusions and intrusions are very small. It will increase the interface energy and decrease the melting point of the deformed solid surface dramatically [14]. Based on Eqn. 41 in reference 14, the drop of the melting point, ΔT , is:

$$\Delta T = 2\Gamma(1/R_d - 1/R_o) \quad (12),$$

where Γ is the Gibbs-Thomson coefficient ($\Gamma = \sigma T_m / \rho L_m$), and R_d and R_o are the radii of the curvatures of the deformed surface and the original surface, respectively. If the radii of the curvatures of the slip band extrusion and intrusion and the original surface are $0.4 \mu\text{m}$ and $2 \mu\text{m}$, respectively, the drop of the melting point will be 3.5K . It is evident that the slip band extrusion and the brim of the intrusion will be remelted or eroded soon. So a new and more curved surface will formed, as shown in Fig. 4.

In isothermally stirred semisolid slurries, this erosion process will gradually erode the roots of the dendrite arms and break them sooner or later. While in continuously stirred cooling semisolid slurries, the



Fig. 4 Sketch of the erosion process at the root of dendrite arms.

undercooled liquid takes away latent heat. The erosion of the solid surface at the roots of the dendrite arms has to race with the growth of the solid surface. Because the erosion rate is proportional to the size of the slip band extrusions and intrusions as well as the bending frequency, as the length of the dendrite arms, L_{arm} , the fluid force, F , and the bending frequency, F_{HZ} are increased; the erosion rate will increase. The erosion rate can be described as:

$$V_{erosion} = K(T)f_1(L_{arm})f_2(F)f_3(F_{HZ}) \quad (13),$$

where $K(T)$ is a factor relates to the remelting of the slip band extrusions and intrusions. As the undercooled system takes away the heat of the liquid in front of the solid-liquid interface, the internal friction heat of plastic deformation offsets the lose. So the growth of the solid surface at the root of the dendrite arms is promoted by high cooling rate, $\partial T/\partial t$, but is hindered by severe plastic deformation. The growth rate of the solid surface can be described as:

$$V_{growth} = f_4(\partial T/\partial t - k\mathcal{E}) \quad (14),$$

where $k\mathcal{E}$ is a term relates to internal friction heat. When $V_{erosion}$ is larger than V_{growth} , the surface at the root of the dendrite arms will be gradually eroded.

5. Conclusion

This simulation indicates that in a moderately stirred semisolid suspension, stress concentration at the roots of the dendrite arms is so great that plastic deformation is easy to occur there. It is thought that the slip band extrusion and intrusion on the skin of the root will decrease the melting point of the solid surface and cause erosion. If the erosion rate of the solid surface of the root is larger than the growth rate of the surface, the root will be gradually eroded and finally ruptured.

6. Acknowledgement

The invaluable support of National Research Laboratory (NRL) Program of Thixo-Rheo Forming and the invaluable financial support of the Ministry of Science & Technology (MOST) are greatly

appreciated.

Reference

- [1] Flemings M.C., "Behavior of Metal Alloys in the Semisolid State", Metall. Trans. A. 1991; 22; 957-981.
- [2] Kirwood D.H., "Semisolid Metal Process", Inter. Mater. Rev. 1994; 39; 173-188.
- [3] Garabedian H., Strickland-Constable R.F., "Collision breeding of ice crystals", J. Cryst. Growth 1974; 22; 188-192.
- [4] Mullis A.M., Battersby S.E., Fletche H.L., "Semi-solid processing of the analogue casting system $\text{NH}_4\text{Cl-H}_2\text{O}$ ", Scripta Mater. 1998; 39; 147-152.
- [5] Apaydin N., Prabhakar K.V., Doherty R.D., "Microstructure of Stir-cast Metals", Mater. Sci. Eng. 1980; 46; 145-150.
- [6] Yang Z., Zhang H.F., Wang A.M., Ding B.Z., Hu Z.Q., "Rheocast structure in a hypoeutectic high chromium white iron": Mater. Sci. Eng. A. 2003; 343; 251-257.
- [7] Mullis A.M., "Growth induced dendritic bending and rosette formation during solidification in a shearing flow" Acta Mater. 1999; 47; 1783-1794.
- [8] Tönhardt R., Amberg G: "Phase-field simulation of dendritic growth in a shear flow" J. Cryst. Growth 1998; 194; 405-425.
- [9] Pilling J., Hellowell A., "Mechanical Deformation of Dendrites by Fluid Flow", Metall. Trans. A 1996; 27; 229-232.
- [10] Cook N.H., "Mechanic and Materials For Design", New York. McGraw-Hill Book Company, 1984; p208, 238.
- [11] Doherty R.D., Lee H.I., Feest E.A., "Microstructure of Stir-cast Metal", Mater. Sci. Eng. 1984; 65; 181-192.
- [12] Lee J.I., Kim G.H., Lee H.I., "Generation of dislocations and subgrains in stir cast Al-6.2Si alloy during semisolid state processing": Mater. Sci. Technol. 1998; 14; 770-775.
- [13] Meguid S.A.: Engineering Fracture Mechanics. London and New York. Elsevier Science Publishers LTD; 1989, p73.
- [14] Trivedi R., Kurz W., "Dendrite growth": Inter. Mater. Rev. 1994; 39; 49-74.
- [15] Hatch J.E., "Aluminum Properties and Physical Metallurgy", USA. American Society for Metals; 1984, p1.